Hydrobiologia (2009) 629:169–186
DOI 10.1007/s10750-009-9769-x

Using bio-optics to investigate the extent of coastal waters: A Swedish case study

Susanne Kratzer · Paul Tett

Published online: 29 April 2009

Abstract In order to develop an optical model to map the extent of coastal waters, the authors analyzed variations in bio-optical constituents and submarine optical properties along a transect from the nutrient-enriched coastal bay, Himmerfjärden, out into the open Baltic Sea. The model is a simple implementation of the "ecosystem approach," because the optical constituents are proxies for important components of ecosystem state. Yellow substance or colored dissolved organic matter (CDOM) is often a marker for terrestrial freshwater or decay processes in the littoral zone. Phytoplankton pigments, especially chlorophyll *a*, are used as a proxy for phytoplankton biomass that may be stimulated by fluvial or coastal inputs of anthropogenic nutrients. Suspended particulate matter (SPM) is placed in suspension by tidal or wind-wave stirring of shallow seabeds, and is therefore an indicator for physical forcing. It is the thesis of this article that such constituents, and the optical properties that they control, can be used to provide an ecological definition of the extent of the coastal zone. The spatial distribution of the observations was analyzed using a steady-state model that assumes diffusional transport of bio-optical variables along an axis perpendicular to the coast. According to the model, the resulting distribution along this axis can be described as a low-order polynomial (of order 1–3) when moving from a "source" associated with land to the open-sea "sink." Order 1 implies conservative mixing, and the higher orders imply significant biological or chemical processes within the gradient. The analysis of the transect data confirmed that the trend of each optical component could be described well using a low-order polynomial. Multiple regression analysis was then used to weigh the contribution of each optical component to the spectral attenuation coefficient $K_d(490)$ along the transect. The results showed that in this Swedish Baltic case study, the inorganic fraction of the SPM may be used to distinguish between coastal and open-sea waters, as it showed a clear break between coastal and open-sea waters. Alternative models may be needed for coastal waters in which fronts interrupt the continuity of mixing.

Guest editors: J. H. Andersen & D. J. Conley
Eutrophication in Coastal Ecosystems: Selected papers from the Second International Symposium on Research and Management of Eutrophication in Coastal Ecosystems, 20–23 June 2006, Nyborg, Denmark

S. Kratzer (✉)
Department of Systems Ecology, Stockholm University, 106 91 Stockholm, Sweden
e-mail: susanne.kratzer@ecology.su.se

S. Kratzer
Department of Physical Geography and Quaternary Geology, Stockholm University, 106 91 Stockholm, Sweden

P. Tett
School of Life Sciences, Napier University, 10 Colinton Road, Edinburgh EH10 5DT, Scotland, UK

Keywords Bio-optics · Coastal zone · Ecosystem approach · Spectral diffuse attenuation coefficient · Diffusion mixing · Optical case 2 waters

Introduction

The coastal zone forms the transition between land and the open sea. Management of the health of ecosystems in this region is important because they are the parts of the sea first impacted by pollution from land and most visible to humans, as well as providing nurseries for young fish and sites for mariculture. States define the width of the coastal zone in different ways: during early modern times, the width was, typically, 3 miles that could be commanded by a land-based, muzzle-loaded, cannon. The twentieth century saw territorial waters expand wider and fisheries limits move offshore, reaching 200 nautical miles or the outer limits of the continental slope in the 1982 UN Convention on the Law of the Sea (UNCLOS, 1982).

During the second half of the century, the quality of coastal water began to seem important, but was initially regulated through the control of discharges only, with little attention paid to the management of the coastal zone, in general. This too has begun to change.

The EU Water Framework Directive (WFD; European Communities, 2000) requires that coastal waters of the European Union be maintained at high or good ecological quality status. It defines the coastal zone as reaching from the land to "a distance of one nautical mile on the seaward side from the nearest point of the baseline from which the breadth of territorial waters is measured, extending where appropriate up to the outer limit of transitional waters." Borja (2005) estimated that only about 20% of the continental shelf areas in Europe are covered by the Water Framework Directive.

In some countries or regions, a greater breadth than one nautical mile is assumed: for example, out to 3 miles from a headland–headland baseline in Scotland. In the United States, there are currently several definitions of coastal waters in use. The U.S. Army Corps of Engineers also defines U.S. coastal waters as extending out to a three nautical mile line, but The H. John Heinz III Center for Science, Economics, and the Environment (2002) uses a distance within 25 miles off shore to delineate coastal from open-sea waters.

All these examples show that the breadth of the coastal zone is defined in different ways, but they all have in common that the coastal zone is defined by a fixed distance to the shore. The grounds on which these widths have been set are unclear, and can be taken as largely pragmatic. However, how broad is the coastal zone in principle and which variables can be used as an indicator of coastal waters? In this article, the authors provide a case study that demonstrates how bio-optical measurements and remote sensing can be used to determine the breadth of the coastal zone on the east coast of Sweden with respect to water quality in the Baltic Sea.

Area description

The Baltic Sea may be regarded as a large fjord of the Atlantic Ocean or a large estuary with weak tides (<20 cm) and, in most places, broad shallow margins. The Baltic Sea is characterized by permanent salinity stratification with a brackish surface layer caused by the high freshwater input from rivers and more saline deep and bottom waters coming in from the North Sea. In the Baltic Proper, the halocline ranges between 40 and 70 m depth. During spring and summer, a seasonal thermocline at depths between 15 and 20 m develops in most parts of the Baltic Sea, providing another density barrier for vertical exchange (Voipio, 1981). The winter water formed during the preceding winter remains as a layer on top of the primary halocline. When the thermocline rises toward the surface, local upwelling can be observed: cold water from below the thermocline is lifted upward and eventually reaches the surface, where it replaces the well-mixed and warmer upper layer (Gidhagen, 1987). In the Baltic Sea, upwellings are usually found within 10–20 km of the coast, and sometimes spread out in finger-like filaments. Gidhagen (1987) and Krężel et al. (2005) found horizontal temperature differences of up to 10 and 14°K, respectively, within particular upwelling events in the Baltic Sea. Upwelling plays an important role for the coastal plankton communities by transporting nutrients from the deep layer to the euphotic zone with major temperature variations taking place.

In addition to the vertical density stratification, the large fluvial input from the north and the saline input of water from the North Sea also produce a strong horizontal salinity gradient across the whole of the Baltic Sea. The surface salinity decreases progressively from 6 to 8 in the Baltic Sea proper, to 5 to 6 in the Bothnian Sea, down to 2–3 in the Bothnian Bay. The salinity is therefore low compared to other seas, and the large freshwater content is associated with a high content of CDOM. Due to the low tidal range in the Baltic Sea, and the strong salinity stratification, there is relatively little resuspension of sediment. Furthermore, Milliman (2001) pointed out that Scandinavian rivers have extremely low sediment loads compared to other European rivers. This is because most rocks are old (pre-Mesozoic) and difficult to erode.

The typical long-term mean horizontal current field in the surface layers has a weak cyclonic pattern, that is, with anticlockwise rotation (Kullenberg, 1981; Stigebrandt, 2001). This leads to currents from the north along the Swedish coast, and from the south along the Finnish coast. The flow gives rise to many horizontal eddies, which are visible in satellite images (Kahru et al., 1995; Victorov, 1996). From the point of view of remote sensing, the Baltic Sea comprises optical case 2 waters (Morel & Prieur, 1977), in which CDOM and SPM play an important part in light attenuation, in addition to the part played by water itself and phytoplankton pigments.

Himmerfjärden is a fjord-like bay situated in the southern Stockholm Archipelago, just south of 60°N, opening into the Baltic Sea (Fig. 1). With a mean depth of about 17 m, Himmerfjärden is rather shallow and consists of a sequence of basins divided by several sills. The bay and its adjacent waters have been well studied for many years, in part because of concern about nutrient enrichment by urban wastewater (Engqvist, 1996; Savage et al., 2002). Due to the low freshwater input (flushing rate 0.025 d^{-1}) and the presence of several sills, Himmerfjärden has a weak circulation and, as observed generally in the Baltic Sea, there is virtually no tidal influence. Applying the CSST (Comprehensive Studies Task Team) model to Himmerfjärden, the inner basins of Himmerfjärden were shown as potentially phosphorus limited, and may be regarded as "potentially eutrophic," despite comparatively low nutrient loading relative to their volume (Tett et al., 2003). The area is subject to frequently occurring summer blooms of filamentous cyanobacteria, dominated by *Aphanizomenon* sp. and *Pseudanabaena limnetica* (Hajdu et al., 1997), as well as occasional surface blooms of *Nodularia spumigena*, which are often more frequent and more intense in the open Baltic Proper, where they may cover large areas that can be monitored by remote sensing (Kahru, 1997; Subramaniam et al., 2000). The filamentous cyanobacteria are able to fix nitrogen, and are limited by phosphorus in their production. Over the whole year, the total phytoplankton biomass tends to be higher inside Himmerfjärden, whereas from June to August, the total cyanobacteria biomass used to be higher outside Himmerfjärden (Hajdu et al., 1997). The recent introduction of nitrogen removal in the sewage treatment plant (STP, Fig. 1) at the head of the bay, however, has reduced this difference, and stimulated the growth of nitrogen-fixing bacteria inside the bay (Elmgren & Larsson, 2001).

The coastal zone and bio-optical properties

Many of the pressures on water quality in the coastal zone originate on land or at the land–sea boundary, and this boundary can be treated as the source for a number of optical constituents in sea water. These constituents are the following:

I. Yellow substance or colored dissolved organic matter (CDOM), which is often a marker for terrestrial freshwater or decay processes in the littoral zone;
II. Phytoplankton pigments, especially chlorophyll *a*, but also carotenoids, provide proxies for phytoplankton biomass, including that which may be stimulated by fluvial or coastal inputs of anthropogenic nutrients; and
III. Suspended particulate matter (SPM) placed in suspension by tidal or wind-wave stirring of shallow seabeds, which is, therefore, an indicator for physical forcing.

These three optical variables determine the diffuse attenuation and, therefore, the light field, and thus may influence the productivity in the sea. Hence, the spectral diffuse attenuation coefficient, $K_d(490)$, can be used to determine the light conditions for phytoplankton or phytobenthic growth. It has also been shown that $K_d(490)$ can be estimated reliably from

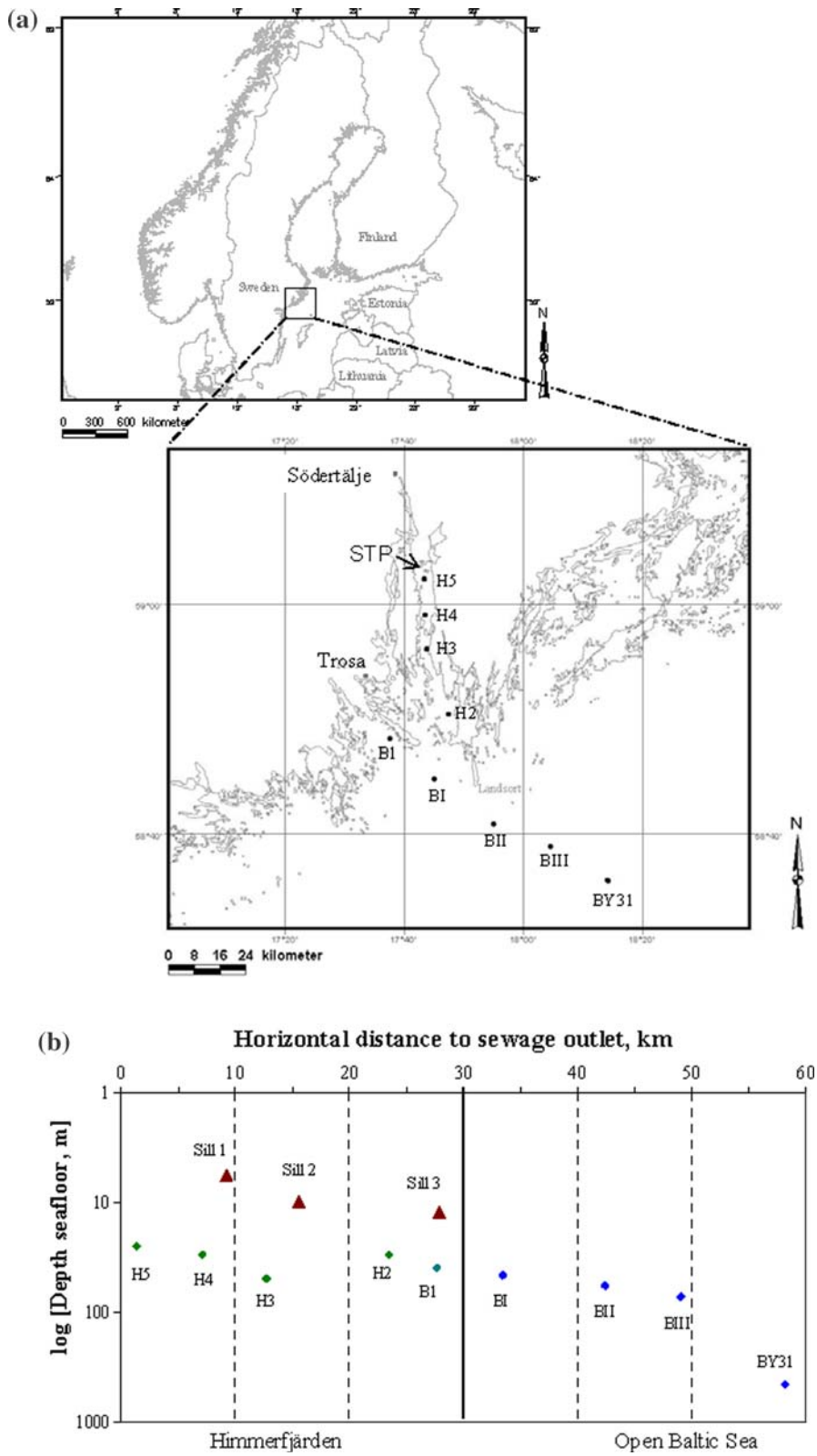

Fig. 1 (**a**) *Top*: Map of Himmerfjärden and adjacent areas. The transect stations are marked on the map. H2–H5, B1 ad BY31 are standard monitoring stations. BY31 is Landsort Deep, the deepest part of the Baltic Sea (459 m). The *arrow* indicates the outlet of the Himmerfjärden Sewage Treatment Plant (STP) close to station H5. (**b**) *Bottom diagram*: Sea floor depth (logarithmic scale) of the transect stations plotted against horizontal distance to the outlet of the sewage treatment plant. The depths of the sills separating the different basins in Himmerfjärden are marked as *triangles*. The line 30 km off the sewage outlet marks roughly the end of coastal waters, and the beginning of open-sea waters as a visual help for analyzing the diagrams

remote sensing observations in the Baltic Sea (Kratzer et al., 2003; Darecki & Stramski, 2004). Furthermore, point estimates of this attenuation coefficient can be obtained from Secchi depth (Kratzer et al., 2003; Pierson et al., 2008). Thus, $K_d(490)$ provides a link between laborious measurements of in-water properties and a variable that can, in principle, be easily mapped over wide areas and thus show the spatial extent of the coastal zone.

It is the thesis of this article that the optical components of sea water, and the optical properties that they control, can be used to map the extent of the coastal zone. This is because they are not only real and important components of marine ecosystems but may also be seen as proxies for some aspects of ecosystem state, and so have the potential to provide a measure of coastal influence that takes account of the "ecosystem approach" instead of the muzzle velocity of a cannon (i.e., instead of the more pragmatic approach based on how far a cannon ball flies). In order to synthesize the effects of these three coastal influences along an axis at right-angles to the shore, we will now look at the contributions of each component to the value of the spectral diffuse attenuation coefficient of downwelling light—$K_d(490)$.

Distribution of optical variables perpendicular to the coast

Two classes of distribution (along an axis perpendicular to the coastline) can be envisaged: continuous and discontinuous. Discontinuous cases include those where hydrodynamic processes create fronts. Shelf-break fronts limit shelf–ocean exchange (Huthnance, 1995) and may thus define the outer boundary of the coastal zone on a narrow shelf. On the broad western Scottish shelf, the haline fronts which form the boundary of the Scottish Coastal Current (Simpson & Hill, 1986) constrain the westward mixing of radiocesium from the Irish Sea (McKay et al., 1986). Fronts separate estuarine plumes from adjacent seas (Garvine, 1986). Even in the absence of obvious fronts, there are often zones in which mixing along the onshore–offshore axis is diminished. Tett et al. (2003) used a box model that assumes complete mixing within a box representing a fjord or enclosed bay, so that the main physical control on flushing time is the limited exchange across the mouth of these "regions of restricted exchange." Such a model was applied to Himmerfjärden bay. Within the bay, advective circulation is weak, and water residence times have been estimated to be upward of 20 days (Engqvist, 1996), increasing with water depth and distance to the mouth of Himmerfjärden. A better model for the distributions of substances along a longitudinal transect originating in the bay would involve spatially continuous eddy-diffusive processes. Box 1 contains solutions for several models of this sort, and suggests that the relationship between a land-derived substance and distance offshore should be that of a polynomial of order 1–3. The first-order polynomial refers to conservative mixing between a nearshore source of a tracer and an offshore sink for the same tracer, and in this case, there will be no obvious break between the nearshore and offshore conditions. The higher-order polynomials result from significant biological or chemical processes along the transect, and in these cases, it may be possible to draw the boundary between coastal and offshore waters at the point where the gradient of the polynomial begins to increase. In any case, even if it is not possible or desirable to make such distinctions, the approach outlined in this mathematical treatment is likely to prove helpful in devising simple models for the coastal region and, in particular, in identifying boundary conditions for them.

Materials and methods

Observations were made along a transect from the head of Himmerfjärden to a station in the Landsort Deep in the deepest part of the Baltic Sea (Fig. 1). The line of stations shown in Fig. 1 extended from H5, near the discharge of a large STP into the Himmerfjärden, to BY31 in the Landsort Deep, with a seabed depth of 459 m. Geophysical and optical variables were measured at these stations during field campaigns in June 2001 and August 2002 (Table 1). GPS positions (GARMIN, GPSMAP, datum: WGS-84) were recorded for each station and used to calculate distances from the wastewater discharge.

The Secchi depth was measured at each transect station (Table 1) using a standard 30-cm white Secchi Disk. A water telescope (collapsible bathyscope,

Table 1 Dates and locations for all optical transect stations in 2001 and 2002 ($n = 34$)

Date	Transect	Location
20–06–2001	Himmerfjärden	H5 – H4 – H3 – H2 – B1
28–06–2001	Open Baltic Sea	B1 – BI – BII – BIII – BY31
02–07–2001	Himmerfjärden/Open Baltic Sea	H4 – H3 – H2 – B1 – BI
04–07–2001	Open Baltic Sea	B1 – BII – BY31
09–08–2002	Open Baltic Sea	BY31 – BIII – BII – BI
12–08–2002	Himmerfjärden	H5 – H4 – H3 – H2
15–08–2002	Open Baltic Sea	BY31 – BIII – BII – BI
22–08–2002	Himmerfjärden	H5 – H4 – H3 – H2

Nuova Rade) was used to avoid the influence of reflectance at the sea surface having an effect on the viewer's reading. The spectral attenuation coefficient $K_d(490)$ was measured with a radiometric system (TACCS, Satlantic Inc.) that included a chain of four sensors for downwelling irradiance at 490 nm ($E_d(490)$) with a 10-nm bandwidth. The sensors were fixed on a cable at 2, 4, 6, and 8 m depths. The instrument was set to record for 2 min at a rate of 1 sample per second, having first been allowed to float 10–20 m away from the boat to avoid shading. The natural logarithm of the measured downwelling irradiance was plotted against depth and the slope of the line taken as $K_d(490)$. During three transects in 2001, the absorption at 440 nm (a_{440}) was measured in situ with an AC9plus (Wetlabs, USA) at 1–2 m below the surface.

Salinity was measured using a SAIV/AS STD which was lowered to a depth of about 14 m. Surface water samples were taken by bucket and used to check surface temperature by measurement with a hand-held thermometer as well as analysis for optical constituents.

Concentrations of organic and inorganic SPM were measured in triplicate by gravimetric analysis using the method of Strickland & Parsons (1972). Kratzer (2000) showed that the gravimetric method to derive SPM had an error of 10% for 29 Baltic Sea duplicates sampled in different bottles.

For the determination of CDOM, the water was filtered through 0.2-µm membrane filters and measured spectrophotometrically (300–800 nm) in a 10-cm optical cuvette using a Shimadzu UVPC 2401 spectrophotometer. The optical density (OD), i.e., absorbance, at 440 nm was corrected for the OD at 750 nm, and g_{440}, the absorption coefficient for CDOM at 440 nm, was derived as follows:

$$g_{440} = \ln(10) \times (\mathrm{OD}_{440} - \mathrm{OD}_{750})/L\ (\mathrm{m}^{-1}),$$
Kirk (1994),

where L is the path length of the cuvette in meters (in this case 0.1 m).

For the estimation of photosynthetic pigments, the spectrophotometric method was applied (Jeffrey & Humphrey, 1975; Parsons et al., 1984), using GF/F filters and extraction into 90% acetone. Chlorophyll *a* was calculated according to the trichromatic method (Parsons et al., 1984) that uses the absorption at 664, 647, and 630 nm, corrected for the reading at 750 nm to account for particle scattering. The algorithm used has shown best results when comparing spectrophotometric methods to high-performance liquid chromatography (HPLC) (Jeffrey & Welschmeyer, 1997), and is also included in the MERIS protocols (Doerffer, 2002). Total carotenoids were estimated according to Parsons et al. (1984), using the absorption at 480 and 510 nm, also corrected for the reading at 750 nm. All laboratory methods followed a standard protocol (Kratzer, 2000; Kratzer et al., 2000). Kratzer (2000) showed that the trichromatic method to derive chlorophyll had an error of 7% for 27 Baltic Sea duplicates sampled in different bottles. An international chlorophyll intercalibration exercise was coordinated by the Norwegian Institute of Water Research (NIVA) for the MERIS validation team in 2002; it included both HPLC and spectrophotometric measurements. The results of the intercalibration (Sørensen et al., 2003) showed that our spectrophotometric chlorophyll measurements of natural water samples were within 8.6% of the median value of the international group. The coefficient of variation for the results reported was 5% between the laboratories (one out of eight laboratories used the fluorometric method). There were 11 laboratories using HPLC

measurements, and the overall coefficient of variation between the laboratories was 14%.

Trend analysis—investigating the applicability of the models described in Box 1

Various types of least-squares regression were used to explore the relationships between the values of the optically active constituents and distance from the wastewater outfall, and to check the applicability of the models described in Box 1. Preliminary statistical analysis showed that when comparing the data sets from 2001 and 2002, there were no significant differences in any of the variables measured; therefore, all data were analyzed together. First-, second- and third-order polynomials were fitted using Excel, and the value of the coefficient of determination (r^2) was used to decide which order of polynomial to use.

Results

Water samples

During the field campaign in June 2001, the weather was unstable. Air temperature ranged from 12.1 to 23.1°C, and only seven out of 18 transect stations were observed under cloud-free conditions. Filamentous cyanobacteria were visible by eye, but did not form any surface accumulations during the period of investigation.

In August 2002, the weather was dominated by high pressure. Air temperature ranged from 21 to 27.3°C, and all 17 transect stations were measured under blue skies (sometimes hazy) and with calm seas. Prior to the field campaign (10–17 July 2002), there had been occurrences of cyanobacteria blooms in the open Baltic Sea area, and later during our field campaign, an increase in filamentous cyanobacteria surface accumulations was again observed. The measured salinity (average over 1–2 m depth) ranged from 5.05 to 6.11 ($n = 27$) at the transect stations in 2001 and 2002.

In most of the following diagrams, measured variables are plotted against distance from the outlet of the STP, which is treated as a significant source of terrestrial properties and thus as the nominal starting point of the transect. Figure 2 shows that surface temperature was relatively constant over each individual transect, but increased progressively over time with the establishment of the seasonal thermocline. As shown in Figs. 3–6, most other variables showed decreasing values with offshore distance, although salinity and Secchi depth increased, and organic SPM (SPOM) showed no simple pattern. There were no obvious abrupt discontinuities in the distributions.

The results of the trend analysis are shown in Table 2. If the difference in r^2 was not significant, then the lower order polynomial was chosen to describe the trend (highlighted equations in Table 2). The results confirm the polynomials derived in Box 1 and show that in most cases, a quadratic equation gave as good a fit as a cubic equation, except for CDOM and salinity, for which a cubic equation provided a significant improvement in explained variance. Amongst significant relationships, the proportion of explained variance was lower for pigments (41–43%) than for CDOM, SPM, inorganic SPM (SPIM), and salinity (69–83%).

Relationships among the variables

Not unexpectedly, there was a considerable correlation among the variables (Table 3), the most marked including an inverse correlation between salinity and CDOM with a correlation coefficient (r) of −0.85 ($n = 26$). There were also very strong correlations

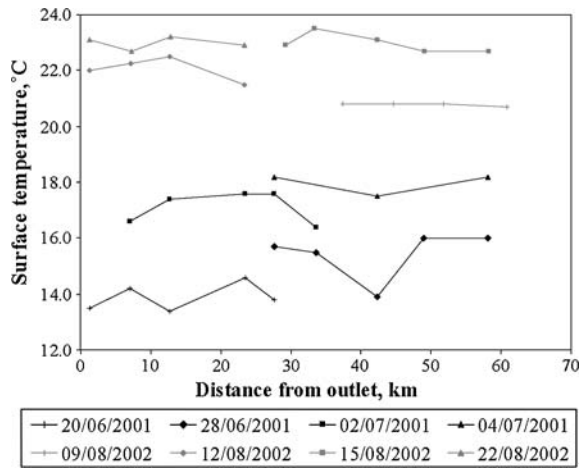

Fig. 2 Horizontal surface temperature profiles measured at the transect stations are shown in Table 1. The temperature transects did not show a difference between coastal and open sea waters. The increase in water temperature was mostly caused by the seasonal trend

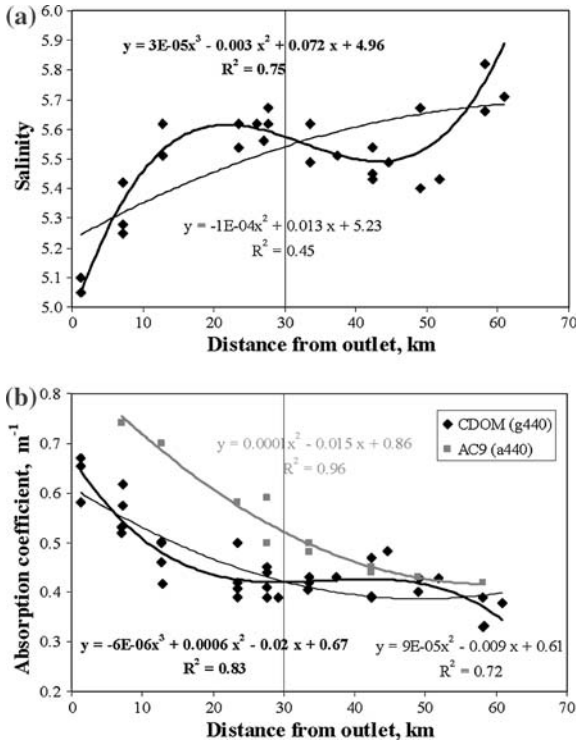

Fig. 3 Transects of **a** salinity and **b** CDOM with polynomial trendlines of second and third order; and including the total absorption at 440 nm, a_{440}, as derived from the AC9. The *vertical line* at 30 km marks the approximate transition from Himmerfjärden to the open Baltic Sea (between B1/Sill 3 and BI)

between $K_d(490)$ and total SPM ($r = 0.88$, $n = 34$), and between chlorophyll and the total carotenoid concentration ($r = 0.89$ $n = 34$).

In addition, there was a high correlation between reciprocal Secchi depth (z_S) and $K_d(490)$, corresponding to the relationship:

$$K_d(490) = 0.18(\pm 0.03) + 1.57(\pm 0.12) \times z_S^{-1} \qquad (1)$$

Multiple regression analysis

Multiple regression analysis was used to estimate the contribution of each optical component to $K_d(490)$. For this, the diffuse attenuation coefficient was first corrected by subtracting 0.022 m^{-1}, the diffuse attenuation of water at 490 nm K_w (Smith & Baker, 1981), from each measured $K_d(490)$ value. The corrected attenuation $[K_d(490) - K_w(490)]$ was then regressed against g_{440} and the concentrations of SPM and chlorophyll *a* (chl-*a*). A significant intercept was obtained for total SPM as a regression variable, but not when using the inorganic fraction, SPIM, instead. The best multiple regression was

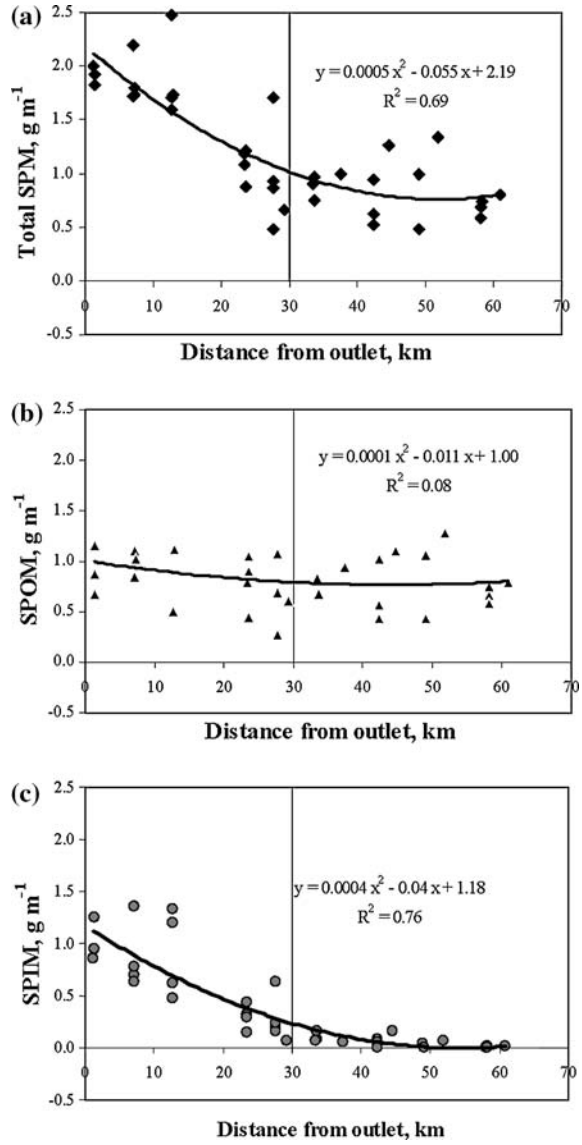

Fig. 4 Transects of **a** SPM load, **b** SPOM load, and **c** SPIM load; all with second order polynomial trendlines

$$[K_d(490) - K_w(490)] = -0.0013 + 0.134 \times [\text{SPIM}] + 0.818 \times g_{440} + 0.0242[\text{chl-}a] \qquad (2)$$
$$r^2 = 0.87,\ p = 0.000,\ n = 34$$

(Using a value of 0.016 m^{-1} for $K_w(490)$, as suggested by Mueller (2000), gave a larger negative intercept of −0.0047, and was rejected.) Analysis of variance for the dataset showed that 49% of the variance in the multiple regression was explained by

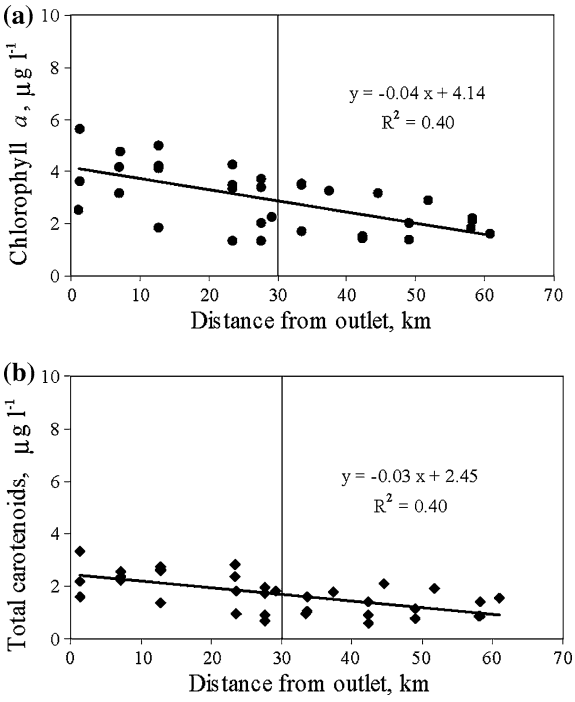

Fig. 5 Transects of **a** chlorophyll *a* concentrations and **b** total carotenoid concentrations, with second order polynomial trendlines

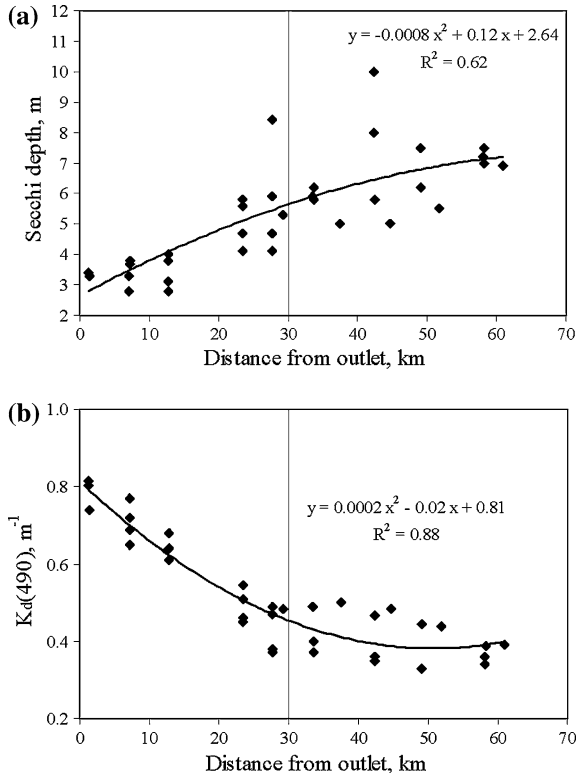

Fig. 6 Transects of **a** Secchi depth and **b** $K_d(490)$ with second order polynomial trendlines

SPIM, 11% by CDOM, and only 2% by chlorophyll. The remainder (38%) was caused by the variability of the optical properties of the three components.

In order to test the influence of chlorophyll on CDOM concentration, we did a multiple regression analysis of g_{440} on salinity and chlorophyll. The regression of g_{440} on salinity explained 69% of the variance, and the regression including chlorophyll explained 77%; so the chlorophyll explained 8% of the variance of g_{440}, and therefore had a significant influence on CDOM.

Synthesis—a coastal attenuation model

Finally, smoothed values of CDOM g_{440} and concentrations of SPIM and chlorophyll at 5 km steps away from the STP were calculated from the polynomial regression equations in Table 2. The coefficients from the multiple regression analysis were then used to weigh the contribution of each optical component to $K_d(490)$. The result of this analysis is shown in the model in Fig. 7d. This coastal model serves as a synthesis and summary of the results of this study.

The model shows that CDOM is optically dominant both in the coastal and the open Baltic Sea stations. SPIM is also optically important within Himmerfjärden, and influences the attenuation up to a horizontal distance of about 40–45 km from the sewage outlet, tending below 0.05 g m^{-3} at about 15–20 km off the coast. Chlorophyll makes a significant contribution to the attenuation in both Himmerfjärden and the open Baltic Sea, with slightly decreasing values away from the land.

Discussion

Observations

The study described here was carried out during the summers of two years—2001 and 2002. Figure 8a and b show the development of the seasonal stratification at station B1 in year 2001 and 2002, respectively. Although two quite different weather conditions were encountered in these years, there

Table 2 Trend analysis for geophysical/optical variables with distance to the sewage outlet

Geophysical parameter	Order polynomial	Polynomial fit ($n = 35$); salinity: $n = 27$	r^2	Adjusted r^2
Temperature	**Quadratic**	$\mathbf{y = 0.0013\ x^2 - 0.0719x + 19.55}$	**0.015**	
Salinity	Quadratic	$y = -0.0001\ x^2 + 0.013\ x + 5.23$	0.449	
	Cubic	$\mathbf{y = 0.00003\ x^3 - 0.003\ x^2 + 0.072\ x + 4.96}$	**0.754**	**0.722**
CDOM	Linear	$y = -0.0036\ x + 0.5583$	0.600	
	Quadratic	$y = 0.00009\ x^2 - 0.009\ x + 0.61$	0.718	
	Cubic	$\mathbf{y = -0.000006\ x^3 + 0.0006\ x^2 - 0.0224\ x + 0.6727}$	**0.826**	**0.809**
SPM	Linear	$y = -0.0231\ x + 1.8769$	0.594	
	Quadratic	$\mathbf{y = 0.0005\ x^2 - 0.055\ x + 2.19}$	**0.685**	**0.666**
SPIM	Linear	$y = -0.0194\ x + 0.9426$	0.678	
	Quadratic	$\mathbf{y = 0.0004\ x^2 - 0.0434\ x + 1.1762}$	**0.762**	**0.747**
SPOM	**Quadratic**	$\mathbf{y = 0.0001\ x^2 - 0.011\ x + 1.00}$	**0.084**	**0.027**
Chl-*a*	**Linear**	$\mathbf{y = -0.0424\ x + 4.1443}$	**0.400**	**0.374**
	Quadratic	$y = 0.0004\ x^2 - 0.067\ x + 4.39$	0.411	
Carotenoids	**Linear**	$\mathbf{y = -0.0253\ x + 2.4518}$	**0.398**	**0.360**
	Quadratic	$y = 0.0004\ x^2 - 0.052\ x + 2.71$	0.432	
Secchi depth	**Linear**	$\mathbf{y = 0.0755\ x + 3.1148}$	**0.602**	**0.577**
	Quadratic	$y = -0.0008\ x^2 + 0.12\ x + 2.64$	0.622	
K_d(490)	Linear	$y = -0.0069\ x + 0.7154$	0.748	
	Quadratic	$\mathbf{y = 0.0002\ x^2 - 0.02\ x + 0.81}$	**0.877**	**0.869**

The polynomial regression with the highest coefficient of determination (r^2) was chosen as the best fit (in bold). The lower-order polynomial was chosen as best fit in the case there was no significant difference in r^2 compared to the higher-order polynomial (in bold)

Table 3 Correlation matrix derived from all transects during summer 2001 and 2002 ($n = 34$) showing the correlation between all optical variables

Mean |r|			Salinity	CDOM	SPM	SPIM	SPOM	Chl-*a*	Carotenoids	Secchi depth
0.54	Salinity	r								
		p								
0.66	CDOM	r	−0.85							
		p	0.000							
0.74	SPM	r		0.71						
		p		0.000						
0.64	SPIM	r		0.68	0.89					
		p		0.000	0.000					
0.46	SPOM	r			0.63					
		p			0.000					
0.58	Chl-*a*	r		0.54	0.59					
		p		0.000	0.000					
0.63	Carotenoids	r		0.53	0.68	0.52		0.89		
		p		0.001	0.000	0.001		0.000		
0.70	Secchi	r		−0.65	−0.88	−0.76	-0.59	−0.61	−0.72	
	depth	p		0.000	0.000	0.000	0.000	0.000	0.000	
0.76	K_d(490)	r	−0.70	0.86	0.88	0.82	0.51	0.64	0.72	−0.86
		p	0.000	0.000	0.000	0.000	0.001	0.000	0.000	0.000

Key to significance level (Fowler et al., 1998):

$p > 0.0011$	No significant correlation
$0.40 \geq \|r\| \leq 0.69$	A modest correlation
$0.70 \geq \|r\| \leq 0.89$	A strong correlation
$0.90 \geq \|r\| \leq 1.00$	A very strong correlation

were no systematic differences between years in any of the optical variables measured.

The value of an optical variable in our model (Fig. 7) can be seen as dependent on (1) the distance offshore, (2) the time of year, and (3) all other factors, treated as noise. An advantage in studying only the summer season was to reduce not only the variability caused by seasonal variations but also the noise, since summer conditions are generally more stable due to the seasonal stratification. However, given that we have proposed a general model for coastal influence but only tested it against a limited dataset, it is necessary to consider whether the optical properties and constituents measured in this particular area of the Baltic Sea during the summers 2001 and 2002 can be considered in any way typical of other summers, other seasons, and other areas in the Baltic Sea.

Table 4 shows that our mean chlorophyll values measured in summer compare well with the HELCOM observations in the Baltic Proper over the period 1994–1998 (HELCOM, 2002). Kratzer et al. (1998) measured optical constituents near Ar at the northern coast of Gotland from 23 July to 5 August 1998 (Table 4). The water here may be considered typical of the northwestern Baltic. The SPM and chlorophyll values observed during 2001/2002 were similar to those at Ar in 1998, whereas the 2001/2002 CDOM values were higher. This can be explained as a result of interannual movements in the north–south trending salinity gradient, and perhaps also by changes in the degree of stratification: in summer 1998, the seasonal thermocline developed only very weakly (Miguel Rodriguez Medina, Baltic Nest Institute, pers. comm., 2007), and few surface accumulations of cyanobacteria were observed (Hansson, 2006).

The seasonal variation of optical components is related to variations in terrestrial runoff. There are two major seasons with high runoff in the Baltic Sea area: in spring, during the thawing period; and in summer, due to the peak of precipitation (Voipio, 1981). An increase in precipitation leads to an increase in terrestrial runoff, which leads to a decrease in salinity (Meier & Kauker, 2003), and an increase in nutrients and humic and fulvic acids. Kowalczuk et al. (2005) investigated CDOM attenuation measured during 39 cruises from 1993 to 2001. They also observed higher values in the coastal areas compared to the open Baltic Sea, and observed higher values in summer than in the autumn/winter period. When comparing the summer to the spring

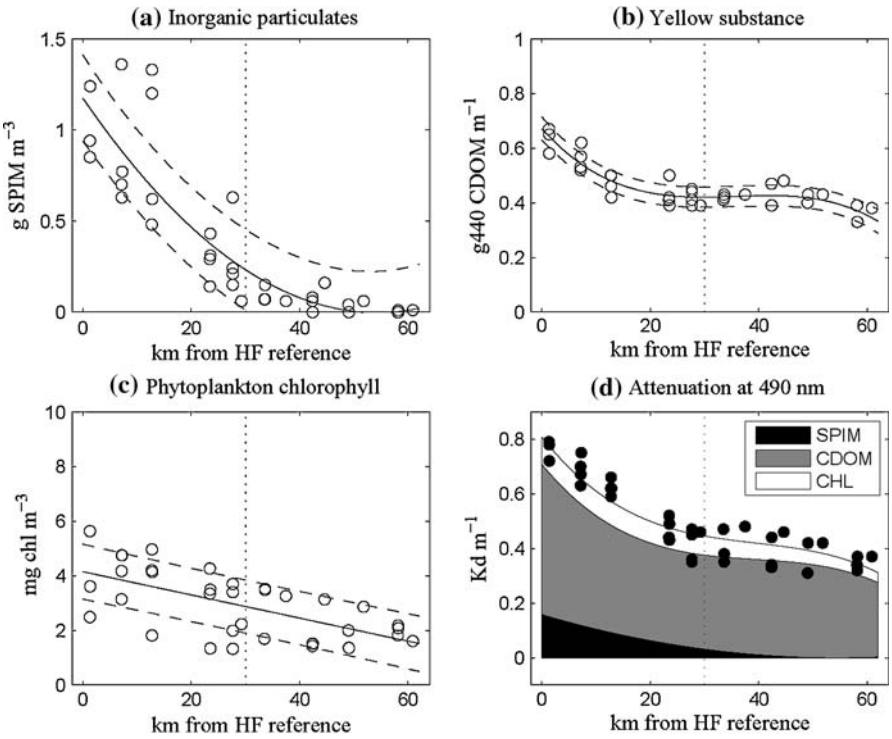

Fig. 7 Best polynomial fit for the concentration of **a** SPIM; **b** CDOM (yellow substance); **c** chlorophyll; and **d** result of the coastal/diffusion model with stacked contributions of each optical component to $K_d(490)$ assuming a polynomial decline of optical constituents in relation to the source (land). The *vertical dotted line* marks the mouth of the Himmerfjärden. The *dashed lines* show confidence limits for the regressions in (**a**)–(**c**). They include at least 50% of possible regressions or up to 68%, if the errors in the *y*-axis variables are normally distributed with constant variance (*graphs* produced in Matlab)

Table 4 Comparison of optical variables in the Baltic Sea by season and geographic area

Area	Season	Mean	SD	Source	Time measured
Chl-*a* (μg l^{-1})					
Baltic Proper	Spring	3.28	4.35	HELCOM (2002)	1994–1998
	Summer	2.51	1.25	HELCOM (2002)	1994–1998
	Autumn	2.07	1.28	HELCOM (2002)	1994–1998
	Winter	0.53	0.47	HELCOM (2002)	1994–1998
Coastal, all stns.	Summer	3.74	2.23	Fig. 5a	Summers 2001/2002
Open Baltic, all stns.	Summer	2.25	0.77	Fig. 5a	Summers 2001/2002
Landsort Deep	Summer	2.15	0.29	Fig. 5a	Summers 2001/2002
Ar, northern Gotland	Summer	2.90	0.59	Kratzer et al. (1998)	23 July–5 August 1998
SPM (g m^{-3})					
Coastal, all stns.	Summer	1.43	0.59	Fig. 4a	Summers 2001/2002
Open Baltic, all stns.	Summer	0.95	0.22	Fig. 4a	Summers 2001/2002
Landsort Deep	Summer	0.73	0.13	Fig. 4a	Summers 2001/2002
Ar, northern Gotland	Summer	0.85	0.25	Kratzer et al. (1998)	23 July–5 August 1998
CDOM, g_{440}					
Coastal, all stns.	Summer	0.48	0.10	Fig. 3b	Summers 2001/2002
Open Baltic, all stns.	Summer	0.40	0.04	Fig. 3b	Summers 2001/2002
Landsort Deep	Summer	0.35	0.03	Fig. 3b	Summers 2001/2002
Ar, northern Gotland	Summer	0.27	0.03	Kratzer et al. (1998)	23 July–5 August 1998
Open sea	Spring	0.34		Kowalczuk et al. (2005)	1993–2004
	Summer	0.32		Kowalczuk et al. (2005)	1993–2004
	Autumn/Winter	0.27		Kowalczuk et al. (2005)	1993–2004
Pomeranian Bay	Spring	0.38		Kowalczuk et al. (2005)	1993–2004
	Summer	0.44		Kowalczuk et al. (2005)	1993–2004

data, it depended on the region whether the summer or the spring values were somewhat higher (Table 4). Unpublished data (Kratzer) suggest that all optical components have higher values in the Landsort Deep in spring than in summer.

Correlations between optical components

It is not surprising that there were significant correlations between some of the optical in-water constituents (Table 3). All would be expected to be correlated insofar as they relate to the common factor of distance and hence obey the diffusion model. However, there are particular links between some of the optical parameters that may explain the correlations: CDOM tends to be high in freshwater and this is likely to explain its good (inverse) correlation with salinity; photosynthetic pigments (chlorophyll and carotenoids) occur together in phytoplankters and are therefore correlated, and chlorophyll might co-occur with suspended particulate organic matter (SPOM) in phytoplankton.

The existence of correlations between variables causes some difficulties in interpreting the results from the multiple regression analysis, and may have biased estimates of the coefficients in Eq. 2. As a check, the coefficients were converted to standardized beam absorption coefficients (a_{490}) by multiplying them by the value of the mean cosine of downward irradiance (μ_0). If one assumes scatter to be negligibly small compared to absorption, then the following relationship may be assumed: $a_{490} = \mu_0 \times K_d(490)$, (Kirk 1994). This is a good assumption at least for open Baltic Sea waters where we have little scatter due to inorganic particles, and where the attenuation is dominated by CDOM absorption. This is exemplified in Fig. 3b, which shows the total absorption of optical constituents (corrected for the absorption by water) at 440 nm measured by the AC9 compared to the CDOM absorption at 440 nm (*Note*: the CDOM measurements

were taken just below the surface, whereas the AC9 integrated the absorption between 1 and 2 m).

Assuming a mean cosine μ_0 of about 0.86 in these waters, the resulting value for chlorophyll (derived from Eq. 2) is 0.021 m^2 $(mg\ chl)^{-1}$, which is an estimate of $a^*_{PH}(490)$, the chlorophyll-specific absorption coefficient at 490 nm. Although realistic in general terms, it is lower than the range of 0.028–0.043 m^2 $(mg\ chl)^{-1}$ (mean = 0.035 m^2 $(mg\ chl)^{-1}$; $n = 12$) reported by Kratzer (2000) for phytoplankton in open Baltic waters in summer 1998, calculated using the filter pad method (Kishino et al., 1985; Cleveland & Weidemann, 1993).

In contrast, the mean cosine-corrected CDOM coefficient in Eq. 2 is 0.70. This coefficient is a dimensionless ratio, $g_{490}/g_{440} = a(\text{CDOM}, 490)/a(\text{CDOM}, 440)$ as the CDOM attenuation was measured at 440 nm, whereas the diffuse attenuation was measured at 490 nm. This ratio is higher than the ratio derived from our measured CDOM spectra, which we estimated to be typically about 0.48. This means that the multiple regression analysis leads to an overestimation of CDOM and an underestimation of chlorophyll attenuation. This problem could be solved mathematically by putting certain constraints on the range of values for each of the variables when performing the multiple regression analysis.

Model fit

To the extent that they are fitted by simple polynomials, the results for most optical constituents and the synthetic variable $K_d(490)$ (Figs. 3–7) are compatible with the diffusion model(s) of Box 1. In these models, the terrestrial end of the transect is a notional source of material and the marine end is a notional sink; the marine sink may be literal in the case of SPIM, which falls close to zero in the water over the Landsort Deep (at BY31). As mentioned in the Results section, SPM and CDOM clearly followed the polynomial decline predicted by the diffusive model, but chlorophyll *a* had a less obvious trend. This may be caused by the dominance of filamentous cyanobacteria during summer: as these are able to fix nitrogen, they are limited by phosphorus (Larsson et al., 2001), and will therefore follow the pattern of phosphate distribution. In the case of, for example, coastal upwelling, and the subsequent replenishment of phosphorus in the surface mixed layer, the biomass of nitrogen-fixing cyanobacteria may start to increase locally offshore, and therefore the smooth gradient—which is described by a polynomial—may be disturbed.

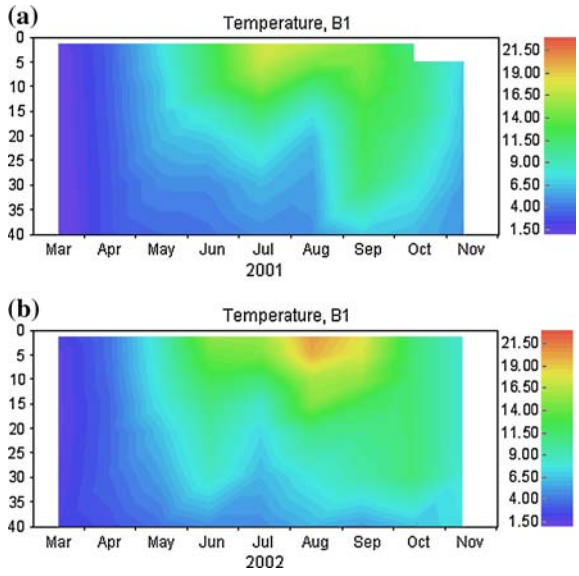

Fig. 8 Development of the seasonal stratification in the top 40 m at Station B1 during the years **a** 2001 and **b** 2002. Images produced by Miguel Rodriguez Medina (using NEST) based on data delivered by the Swedish Meteorological and Hydrological Institute (SMHI) and the Swedish Marine Research Centre (SMF) within the framework of the Swedish Environmental Monitoring Programme (1–2 week sampling)

Upwelling might also lead to an abrupt change in water mass and therefore in the underwater optical characteristics. The presence of upwelling is shown by colder water filaments in some of the sea-surface temperature images in Fig. 9. Gidhagen (1987), Lehmann et al. (2002), and Myrberg & Andrejev (2003) found that the width-scale of upwellings (perpendicular to the coast) in the Baltic Sea is typically in the range of 5–20 km. The occurrence of upwelling in our research area is shown by colder water filaments in some of the sea-surface temperature images shown in Fig. 9, but as shown in the trend lines of Figs. 3–7, there were no abrupt changes in optical constituents in the upwelling areas.

Nevertheless, there is the difficulty of recognizing a discontinuous distribution, or distinguishing between it and a continuous distribution, in the presence of variation. By "continuous" we mean a distribution that is truly described by the simple polynomials dealt with in this article and with shore-normal transports dominated by eddy diffusion at a rate that is either constant

or changes monotonically and smoothly along the transect. By "discontinuous" we mean the type of distribution that would be observed in a case where there was at least one region of the transect in which the coefficient of horizontal eddy diffusion was much lower than in surrounding regions. The discontinuous case would be expected to result in an obvious step in the graphs of optical properties or constituents against distance. The difficulty mentioned above is that of distinguishing such a step amidst the scatter of points shown in these graphs. Although the data we have presented do not refute the existence of discontinuities, these would nevertheless have to be sufficiently small that their step-like effects are confined within the confidence limits shown in Fig. 7. Of course, different conclusions may be reached for other sea areas, especially those where bottom-locked tidal mixing fronts provide significant barriers to offshore transports.

A final point about the model solutions is that they assume (i) a steady state and (ii) constancy of shore-normal gradients along a shore-parallel axis. Bowers (Dave Bowers, School of Ocean Sciences, University of Wales Bangor, pers. comm., 2007) has pointed out that curvilinear relationships can emerge from linear mixing models (order 1 polynomials) when the endmember concentrations change with time (Cifuentes et al., 1990). Our use of data from two summers goes some way to eliminate this possibility, but it is desirable to obtain data from further years to be sure of this. The diffusional models of Box 1 do not require that there be no shore-parallel transports, but only that that the source or sink terms that might result from these crossing a shore-normal gradient should be constant in time and change smoothly along the transect. Remote sensing, as shown in Fig. 10, lends some support to the argument that any

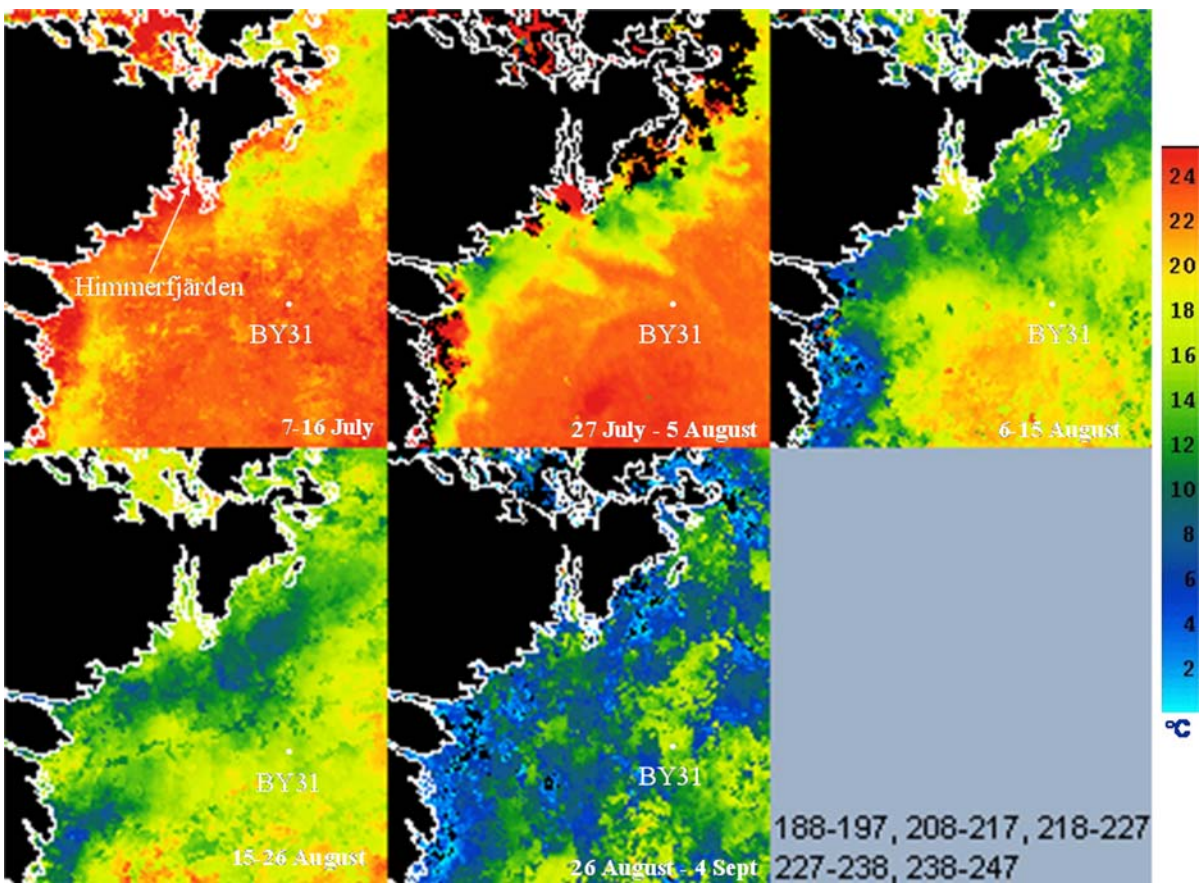

Fig. 9 Remotely sensed sea-surface temperatures of Himmerfjärden and adjacent area derived from NOAA/AVHRR data 7 July–3 September 2001. The 10-day composites reveal temperature differences, most probably caused by upwelling. Data processing by Miho Ishii and Roberta Mistretta. Note that the length of Himmerfjärden is about 30 km

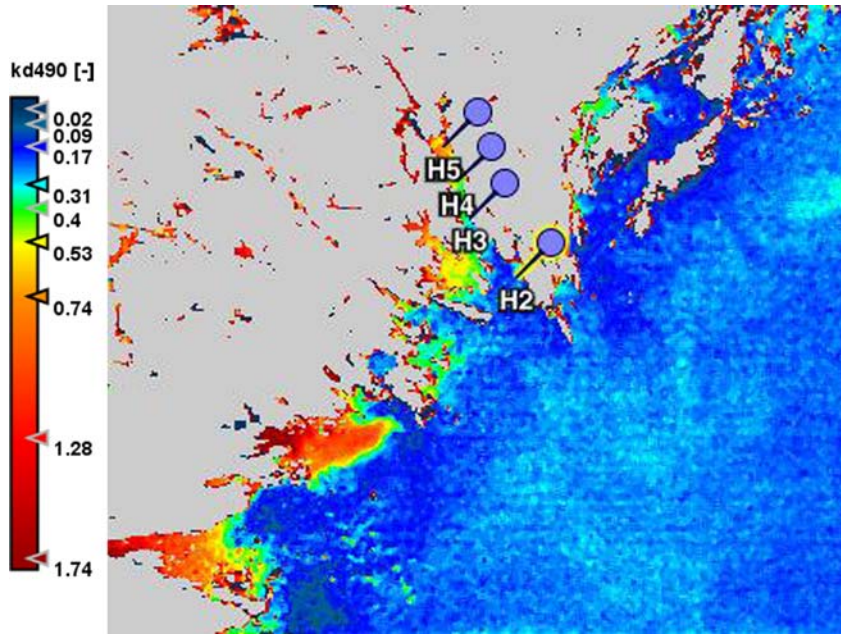

Fig. 10 MERIS $K_d(490)$ full resolution image (300 m resolution) from 22 August 2002 processed using BEAM and the $K_d(490)$ algorithm derived from sea-truthing data (Kratzer et al., 2008)

Box 1 Diffusional model equations

In this one-dimensional, steady-state model, x is the horizontal distance in meters along a transect with origin offshore and terminus at $x = l$. Y is a generalized variable (amount m^{-3}), with boundary conditions of Y_0 at $x = 0$ and Y_l at $x = l$. The defining equation is

$$\frac{\partial Y}{\partial t} = 0 = -K_h \cdot \frac{\partial^2 Y}{\partial x^2} + \beta_y$$

where K_h is a horizontal mixing coefficient ($m^2\ d^{-1}$) and β_Y is the total of biogeochemical and ecological sources and sinks (amount $m^{-3}\ d^{-1}$) at a point on the transect. Solutions depend on assumptions about K_h and β_Y, and it is convenient to write

$$\frac{\partial^2 Y}{\partial x^2} = 2 \cdot k_0 \cdot (1 + a_1 \cdot x + a_2 \cdot x^2 \cdots), \text{ where } k_0 = \frac{\beta_Y(x=0)}{2K_h(x=0)}$$

and the power series allows for spatial variability in rates. A general solution is

$$Y = k_0 \cdot x^2 \cdot \left(1 + \frac{a_1 \cdot x}{3} + \frac{a_2 \cdot x^2}{12} \cdots\right) + b \cdot \frac{x}{l} + Y_o \text{ where}$$
$$b = (Y_l - Y_0) - k_0 \cdot l^2 \cdot \left(1 + \frac{a_1 \cdot l}{3} + \frac{a_2 \cdot l^2}{12} + \cdots\right).$$

The simplest solutions, which neglect all but the zeroth and first-order (a_1) terms of the series, are

Case 1: $a_1 = 0$ and the substance described by Y is conservative, so that $\beta_Y = 0$:

$$Y = (Y_l - Y_0) \cdot \frac{x}{l} + Y_0.$$

Case 2: $a_1 = 0$, and the ratio of β_Y and K_h is positive and constant:

$$Y = \frac{\beta_Y}{2K_h} \cdot x^2 + b_2 \cdot \frac{x}{l} + Y_0, \text{ where } b_2 = (Y_l - Y_0) - \frac{\beta_Y}{2K_h} \cdot l^2.$$

Case 3: a_1 is positive. This would be true where eddy mixing is scale dependent (Okubo, 1974) and so increases offshore (i.e., with $(l - x)$), whereas the non-conservative term β_Y increases as nutrients or stirring increase toward the shore:

$$Y = k_0 \cdot \left(\frac{a_1}{3} \cdot x^3 + x^2\right) + b_3 \cdot \frac{x}{l} + Y_0, \text{ where } b_3 = (Y_l - Y_0) - k_0 \cdot l^2 \cdot \left(1 + \frac{a_1}{3} \cdot l\right).$$

one shore-normal transect can be considered representative of a considerable shore-parallel distance (Box 1).

Conclusion

The aim of this article has been to assess the width of the coastal zone on the basis of selected ecosystem properties that are influenced by coastal or terrestrial processes. We have shown that a diffusional model fits observations from a Swedish coastal water area in summer. An essential feature of the first- and second-order polynomials that fitted chlorophyll and SPM is that they are smoothly monotonic—that is, they contain no obvious discontinuities that can be used to separate nearshore and offshore waters. The CDOM decay was third order and hence provides some evidence of a break.

One obvious place to look for a limit to the coastal influence is at the mouth of the Himmerfjärden, approximately 30 km from the STP. As shown in Fig. 7, this point corresponds to a weak inflexion in the CDOM curve and to the minimum offshore distance at which the 50% confidence limits includes zero. Alternatively, we may look further offshore, at 40–50 km from the STP and 10–20 km from the open coast. It is at this distance that SPIM and chlorophyll concentrations are statistically indistinguishable from those at the "sink" end of the transect, and here that the CDOM curve begins again to descend toward the open-sea endmember value. This is certainly further than the 1 nautical mile limit of the Water Framework Directive.

Considering the low fluvial SPM input in the northwestern Baltic Sea compared to the southern Baltic Sea (Voipio, 1981), with SPM values of up to 15 g m^{-3} (Siegel et al., 2005), one would expect coastal waters to extend even further in the southern Baltic Sea.

In the case of CDOM and salinity, the inflection point at 45–50 km away from the STP and 15–20 km off the coast may be influenced by the upwelling events shown in Fig. 9, and also to a minor extent by the Swedish coastal current that transports water masses from the Bothnian Sea rich in CDOM and lower in temperature down along the Swedish coast. Considering the trendline for CDOM, it is also possible that some of the CDOM pool may be of biological origin and may be produced by phytoplankton (Kowalczuk et al., 2006), or in this case by cyanobacteria. However, as reported in the Results section, chlorophyll explained only a small part of the variance in CDOM (about 8%); therefore, so this explanation seems less likely.

Figure 7d shows how the attenuation coefficient is composed of three optical components: CDOM, SPM, and chlorophyll, and how their concentrations change with distance to the shore. As mentioned in the Introduction, each of the components is an indicator for an important ecosystem property, and thus $K_d(490)$ can serve as an indicator that synthesizes coastal influence as well as being a biologically important variable. Thus, it would seem to be a useful variable with which to map the extent of the coastal zone, and one that embodies the "ecosystem approach."

A robust relationship has been established between water-leaving radiance and $K_d(490)$ (Mueller, 2000) and, to date, $K_d(490)$ has been shown to be the most reliable parameter that can be measured by remote sensing methods (Darecki & Stramski, 2004). A good relationship between $K_d(490)$ and Secchi depth in the Baltic has already been confirmed (Kratzer et al., 2003), and Kratzer et al. (2008) have developed a new $K_d(490)$ algorithm to monitor coastal areas in the northwestern Baltic Sea using MERIS data. Thus, there are old and new tools at hand to apply this approach to estimating the width of the coastal zone.

Acknowledgements This work was funded by the Swedish National Space Board, the EU FP5 project Oceanographic Applications to Eutrophication in Regions of Restricted Exchange (OAERRE), the EU FP6 project Science and Policy Integration for Coastal System Assessment (SPICOSA), and by the Swedish MISTRA program under RESE 5 (Remote sensing for the environment—Methods for detection of changes in aquatic ecosystems and monitoring of algal blooms). Thanks to the Swedish Wallenberg Foundation for an expensive equipment grant. Thanks to Stefanie Hirch, Roberta Mistretta, Antonia Sandman, and Charlotte Sahlin for their help in the field and the laboratory, to Henrik Lindh (SMHI) and the staff of the Askö Laboratory for support during fieldwork. Many thanks to Miho Ishii and Roberta Mistretta for processing the AVHRR data, and to Bertil Håkannsson for his support. Thanks to Paul Sweeny from the U.S. Environmental Protection Agency for information on coastal zone definitions in the USA. Special thanks to Roland Doerffer, Anders Engqvist, Ragnar Elmgren, and Ulf Larsson for discussions and useful comments to the manuscript, and to Miguel Rodriguez Medina for preparing the images of temperature profiles for 2001 and 2002.

References

Borja, A., 2005. The European water framework directive: a challenge for nearshore, coastal and continental shelf research. Continental Shelf Research 25: 1768–1783.

Cifuentes, L. A., L. E. Schemel & J. H. Sharp, 1990. Qualitative and numerical analyses of the effects of river inflow variations on mixing diagrams in estuaries. Estuarine, Coastal and Shelf Science 30: 411–427.

Cleveland, J. S. & A. D. Weidemann, 1993. Quantifying absorption by aquatic particles: a multiple scattering correction for glass-fibre filters. Limnology and Oceanography 38: 1321–1327.

Darecki, M. & D. Stramski, 2004. An evaluation of MODIS and SeaWiFS bio-optical algorithms in the Baltic Sea. Remote Sensing Environment 89: 326–350.

Doerffer, R., 2002. Protocols for the validation of MERIS water products. European Space Agency, Doc. No. PO-TN-MEL-GS-0043.

Elmgren, R. & U. Larsson, 2001. Eutrophication in the Baltic Sea area: integrated coastal management issues. In von Bodungen, B. & R. K. Turner (eds), Science and Integrated Coastal Management. Dahlem University Press, Berlin: 15–35.

Engqvist, A., 1996. Long-term nutrient balances in eutrophication of the Himmerfjärden estuary. Estuarine, Coastal and Shelf Science 42: 483–507.

European Communities, 2000. Water Framework Directive. Directive 2000/60/EC of the European Parliament and of the Council of 23 October 2000 establishing a framework for Community action in the field of water policy. Official Journal of the European Communities L 327: 1–73.

Fowler, J., L. Cohen & P. Jarvis, 1998. Practical Statistics for Field Biology. John Wiley & Sons, Chinchester.

Garvine, R. W., 1986. The role of brackish plumes in open shelf waters. In Skreslet, S. (ed.), The Role of Freshwater Outflow in Coastal Marine Ecosystems. Springer-Verlag, Berlin: 47–65.

Gidhagen, L., 1987. Coastal upwelling in the Baltic Sea – Satellite and in situ measurements of sea-surface temperatures indicating coastal upwelling. Estuarine Coastal and Shelf Science 24: 449–462.

Hajdu, S., U. Larsson & K. Skärlund, 1997. Chapter 9: Växtplankton (Phytoplankton). In Elmgren, R. & U. Larsson (eds), Himmerfjärden. Naturvårdsverket Förlag, Stockholm, Rapport 4565.

Hansson, M., 2006. Cyanobakterieblomningar i Östersjön, resultat från satellitövervakningen 1997–2005. SMHI Rapport 82.

HELCOM, 2002. Environment of the Baltic Sea Area, Baltic Sea Environment Proceedings No. 82B. Helsinki Commission – Baltic Marine Environment Protection Commission.

Huthnance, J. M., 1995. Circulation, exchange and water masses at the ocean margin: the role of physical processes at the shelf edge. Progress in Oceanography 35: 353–431.

Jeffrey, S. W. & G. F. Humphrey, 1975. New spectrophotometric equation for determining chlorophyll a, b, c1 and c2. Biochemie und Physiologie der Pflanzen 167: 194–204.

Jeffrey, S. W. & N. A. Welschmeyer, 1997. Appendix F: spectrophotometric and fluorometric equations in common use in oceanography. In Jeffrey, S. W., R. F. C. Mantoura & S. W. Wright (eds), Phytoplankton Pigments in Oceanography. Monographs on Oceanographic Methodology. UNESCO Publishing, Berlin: 597–615.

Kahru, M., 1997. Using satellites to monitor large-scale environmental change: a case study of cyanobacteria blooms in the Baltic Sea. In Kahru, M. & C. W. Brown (eds), Monitoring Algal Blooms – New Techniques for Detecting Large-Scale Environmental Change. Springer-Verlag, Berlin: 43–61.

Kahru, M., B. Håkansson & O. Rud, 1995. Distribution of sea-surface temperature fronts in the Baltic Sea as derived from satellite imagery. Continental Shelf Research 15: 663–679.

Kirk, J. T. O., 1994. Light and Photosynthesis in Aquatic Ecosystems, 2nd ed. Cambridge University Press, Cambridge.

Kishino, M., M. Takahashi, N. Okami & S. Ichimura, 1985. Estimation of the spectral absorption coefficients of phytoplankton in the sea. Bulletin of Marine Science 37: 634–642.

Kowalczuk, P., J. Olszewski, M. Darecki & S. Kaczmarek, 2005. Empirical relationships between coloured dissolved organic matter (CDOM) absorption and apparent optical properties in Baltic Sea waters. International Journal of Remote Sensing 26: 345–370.

Kowalczuk, P., C. A. Stedmon & S. Markager, 2006. Modelling absorption by CDOM in the Baltic Sea from season, salinity and chlorophyll. Marine Chemistry 101: 1–11.

Kratzer, S., 2000. Bio-optical studies of coastal waters. PhD thesis. School of Ocean Sciences, University of Wales, Bangor.

Kratzer, S., P. Land & N. Strömbeck, 1998. An optical in-water model for the Baltic Sea. Ocean Optics XIV Conference Papers, Vol. 2. New Insights from Ocean Color.

Kratzer, S., D. G. Bowers & P. Tett, 2000. Seasonal changes in colour ratios and optically active constituents in the optical Case-2 waters of the Menai Strait, North Wales. International Journal of Remote Sensing 21: 2225–2246.

Kratzer, S., B. Håkansson & C. Sahlin, 2003. Assessing Secchi and photic zone depth in the Baltic Sea from satellite data. Ambio 32: 577–585.

Kratzer, S., C. Brockmann & G. Moore, 2008. Using MERIS full resolution data to monitor coastal waters – A case study from Himmerfjärden, a fjord-like bay in the north-western Baltic Sea. Remote Sensing Environment 112(5): 2284–2300.

Krężel, A., M. Ostrowski & M. Szymelfenig, 2005. Sea surface temperature distribution during upwelling along the Polish Baltic coast. Oceanologia 47: 415–432.

Kullenberg, G., 1981. Physical oceanography. In Voipio, A. (ed.), The Baltic Sea. Elsevier Oceanography Series 30, Amsterdam.

Larsson, U., S. Hajdu, J. Walve & R. Elmgren, 2001. Estimating Baltic nitrogen fixation from the summer increase in upper mixed layer total nitrogen. Limnology and Oceanography 46: 811–820.

Lehmann, A., W. Krauss & H.-H. Hinrichsen, 2002. Effects of remote and local atmospheric forcing on circulation and upwelling in the Baltic Sea. Tellus 54A: 299–316.

McKay, W. A., M. S. Baxter, D. J. Ellett & D. T. Meldrum, 1986. Radiocaesium and circulation patterns west of Scotland. Journal of Environmental Radioactivity 4: 205–232.

Meier, H. E. M. & F. Kauker, 2003. Sensitivity of the Baltic Sea salinity to the freshwater supply. Climate Research 24: 231–242.

Milliman, J. D., 2001. Delivery and fate of fluvial water and sediment to the sea: a marine geologist's view of European rivers. Scientia Marina 65: 121–132.

Morel, A. & L. Prieur, 1977. Analysis of variations in ocean colour. Limnology and Oceanography 22: 709–722.

Mueller, L. J., 2000. SeaWiFS algorithm for the diffuse attenuation coefficient, K(490), using water-leaving radiances at 490 and 555 nm. In Hooker S. B. & E. R. Firestone (eds), SeaWiFS Postlaunch Calibration and Validation Analyses, Part 3, 11. NASA Goddard Space Flight Center, Greenbelt, MD: 24–27.

Myrberg, K. & O. Andrejev, 2003. Main upwelling regions in the Baltic Sea – A statistical analysis based on three-dimensional modeling. Boreal Environment Research 8: 97–112.

Okubo, A., 1974. Some speculations on oceanic diffusion diagrams. Rapport et Procès-Verbaux des Réunions du Conseil International pour l'Exploration de la Mer 167: 77–85.

Parsons, T. R., Y. Maita & C. M. Lalli, 1984. A Manual of Chemical and Biological Methods for Seawater Analysis. Pergamon Press.

Pierson, D., S. Kratzer, N. Strömbeck & B. Håkansson, 2008. Relationship between the attenuation of downwelling irradiance at 490 nm with the attenuation of PAR (400 nm–700 nm) in the Baltic Sea. Remote Sensing of Environment 112(3): 668–680.

Savage, C., R. Elmgren & U. Larsson, 2002. Effects of sewage-derived nutrients on an estuarine macrobenthic community. Marine Ecology Progress Series 243: 67–82.

Siegel, H., M. Gerth, G. Tschersich, T. Ohde & T. Heene, 2005. Ocean colour remote sensing relevant water constituents and optical properties of the Baltic Sea. International Journal of Remote Sensing 26: 315–330.

Simpson, J. H. & A. E. Hill, 1986. The Scottish coastal current. In Skreslet, S. (ed.), The Role of Freshwater Outflow in Coastal Marine Ecosystems, Vol. G7. Springer-Verlag, Berlin: 195–204.

Smith, R. C. & K. S. Baker, 1981. Optical properties of the clearest natural waters (200–800 nm). Applied Optics 20: 177–184.

Sørensen, K., M. Grung & R. Röttgers, 2003. An intercomparison of in vitro chlorophyll-a determinations. Proceedings of the MERIS Cal/Val Meeting at ESRIN, Frascati, Italy, 10–11 December.

Stigebrandt, A., 2001. Chapter 2: physical oceanography of the Baltic Sea. In Wulff, F., L. Rahm & P. Larsson (eds), A System Analysis of the Baltic Sea. Springer Verlag, Berlin: 19–74.

Strickland, J. H. D. & T. R. Parsons, 1972. A practical handbook of sea-water analysis. Bulletin Journal of the Fisheries Research Board of Canada 167: 185–203.

Subramaniam, A., S. Kratzer, E. J. Carpenter & E. Soderback, 2000. Remote sensing and optical in-water measurements of a cyanobacteria bloom in the Baltic Sea. Proceedings of the Sixth International Conference on Remote Sensing for Marine and Coastal Environments 1: 57–64.

Tett, P., L. Gilpin, H. Svendsen, C. P. Erlandsson, U. Larsson, S. Kratzer, E. Fouilland, C. Janzen, J.-Y. Lee, C. Grenz, A. Newton, J. G. Ferreira, T. Fernandes & S. Scory, 2003. Eutrophication and some European waters of restricted exchange. Continental Shelf Research 23: 1635–1671.

The H. John Heinz III Center for Science, Economics, and the Environment, 2002. The State of the Nation's Ecosystems: Measuring the Lands, Waters, and Living Resources of the United States. Cambridge University Press, Cambridge.

UNCLOS, 1982. United Nations Convention on the Law of the Sea, 10 December 1982.

Victorov, S. V., 1996. Regional Satellite Oceanography. Taylor & Francis, London.

Voipio, A., 1981. The Baltic Sea. Elsevier Science Publishers, Amsterdam.